Microscopic investigation of phonon modes in SiGe alloy nanocrystals

Shang-Fen Ren,[1] Wei Cheng,[1,2] and Peter Y. Yu[3]
[1]*Department of Physics, Illinois State University, Normal, Illinois 61790-4560, USA*
[2]*Institute of Low Energy Nuclear Physics, Beijing Normal University, Beijing, 100875, Peoples Republic of China*
[3]*Department of Physics, University of California, Berkeley, and Molecular Sciences Division, Lawrence Berkeley National Laboratory, Berkeley, California 94720, USA*
(Received 17 December 2003; revised manuscript received 14 April 2004; published 30 June 2004)

Phonon modes in spherical silicon germanium alloy (SiGe) nanocrystals containing up to 1147 atoms (3.6 nm) have been investigated as a function of the Si concentration. Microscopic details of phonon modes, including phonon frequencies and vibrational amplitudes, phonon density-of-states are calculated directly from the dynamic matrices. In particular, the dependence of phonon frequency on the configuration (such as a different ratio of Si to Ge atoms), and location (surface or interior) of clusters of atoms in SiGe alloy nanocrystals have been investigated. Low frequency surface phonons that are related to the spheroidal and torsional modes of a continuum sphere are identified and their frequency dependence on alloy concentration elucidated. The calculated results are compared with measured Raman spectra in bulk, thin films, and superlattices of SiGe alloy reported in the literature. Insights into the behavior of Raman peaks usually identified as Ge-Ge, Si-Si, and Ge-Si optical phonon modes are presented.

DOI: 10.1103/PhysRevB.69.235327 PACS number(s): 81.05.Bx, 63.22.+m, 78.30.−j, 63.50.+x

I. INTRODUCTION

Nanocrystals (NC) of Ge have received a lot of interests in recent years.[1] Often such Ge structures are grown in a Si-rich environment. For example, self-organized quantum dots (QDs) of Ge have been grown on Si substrates by molecular beam epitaxy via the Stranski-Krastanow mode of growth,[2] and NC of Ge have been grown by implantation of Ge ions into SiO_2.[3] Under these growth conditions, interdiffusion between Si and Ge to form an alloy may occur. This interdiffusion has been observed in Si/Ge superlattices[4,5] as well as in Ge QDs grown on Si without a Sb surfactant layer.[2] A sensitive technique to detect the presence of SiGe alloy has been Raman scattering since it has been demonstrated that in bulk SiGe alloy Si produces a local mode with frequency $\sim 410\ cm^{-1}$ in Ge.[6,7] This mode is very well-defined being intermediate in frequency between the optical phonons in pure Ge (at $\sim 300\ cm^{-1}$) and pure Si (at $\sim 520\ cm^{-1}$). In addition to this local mode, alloying also results in shifts and broadening of the Si and Ge optical phonon peaks relative to that of the pure materials.[6,7] The alloying effects can sometimes interfere with the use of Raman scattering to study the effect of strain and confinement of phonon modes in Ge NC since both strain and confinement can produce a red-shift of the Ge optical phonon similar to that due to alloying.[2] Thus it is desirable to investigate other effects of confinement, such as the effect on the local phonon modes, the formation of surface modes, and the effect of alloying on the Raman spectra of Ge NC.

In this paper, we have calculated phonon modes of spherical SiGe NC containing up to 1147 atoms (diameter $d \sim 3.6$ nm). These NC are assumed to have a free surface and the alloy atoms to be randomly distributed for varying amounts of Si. We have investigated the effects of alloying and confinement on the phonon density-of-states (PDOS). The results are compared with available experimental Raman measurements in bulk and NC SiGe alloys.

This paper is organized as the follows: In Sec. II, the theoretical model is described briefly. In Sec. III, the theoretical results are presented. In Sec. IV, the results are discussed and compared with available experimental measurements. Finally in Sec. V, we summarize and conclude.

II. THEORETICAL APPROACHES

The theoretical model used in this research is a valence force field model[8] that we have developed in recent years to calculate phonon modes in semiconductor QDs and NC (for the purpose of discussing their vibrational modes we will make no distinction between QD and NC in this paper).[9–15] In all these previous studies, reasonable agreements between theory and available experimental data were found. This model has also been employed successfully to study surface phonons in Ge NC.[15] This paper extends these previous studies to NC of semiconductor alloys.

In this model, the change in the total energy of an elemental semiconductor, such as Si or Ge, due to lattice vibration is described by the following equation:[8]

$$\Delta E = \sum_i (1/2) C_0 (\Delta d_i / d_i)^2 + \sum_j (1/2) C_1 (\Delta \theta_j)^2, \qquad (1)$$

where C_0 and C_1 are the bond stretching and the bond bending force constants, respectively. The summation in Eq. (1) runs over all the bond lengths and bond angles inside the NC. Because both of these two parameters have a simple and clear physical meaning, this model allows us to treat the interaction between atoms near and at the surface appropriately. By using this model, the microscopic details of the phonon modes, including both the vibrational frequencies and atomic vibrational strengths, are obtained directly from the dynamic matrices. However, because of its simplicity, this model does not fully agree with experimental data in terms of predicting correctly both the bulk sound velocities

and the zone boundary acoustic phonon frequencies. One should keep this in mind in interpreting the results of our calculations.

In the present work, this model is generalized to study the random binary alloy SiGe using the mass-difference-only approximation. In this approximation, the force constants for both Si atoms and Ge atoms are assumed to be the same, and they are taken to be equal to the force constants of bulk Ge: $C_0=47.2$ eV and $C_1=0.845$ eV.[8] In the mass-difference-only approximation, the difference in the bulk Si and Ge optical phonon frequencies results from their different masses ($m_{\mathrm{Si}}=28.1$ au and $m_{\mathrm{Ge}}=72.6$ au) and different lattice constants ($a_{\mathrm{Si}}=5.43$ Å, and $a_{\mathrm{Ge}}=5.63$ Å). The highest Si bulk optical phonon frequency calculated in this approximation is 502 cm^{-1}, which differs from the experimental value of 520 cm^{-1} by only 3%, which suggests that this is a reasonably good approximation.

In our calculations, we further assume that the Si atoms are randomly distributed within the NC, and there is no ordering of any type in the NC. In particular, there is no long-range ordering of the Si and Ge atoms which have been found experimentally to give rise to well-defined Raman peaks around 255 and 435 cm^{-1}.[16] Since Si and Ge bulk materials have different lattice constants, the lattice constant of the alloy $\mathrm{Si}_x\mathrm{Ge}_{1-x}$ is approximated by an interpolation between those of Si and Ge using Vegard's law[17]

$$a_{\mathrm{SiGe}} = xa_{\mathrm{Si}} + (1-x)a_{\mathrm{Ge}}, \tag{2}$$

where a_{Si} and a_{Ge} are, respectively, the lattice constants of Si and Ge, and x is the silicon fractional concentration. We typically start from a small NC that is approximately spherical in shape. We fix the numbers of Si and Ge atoms and run the computer programs many times with different random locations of the Si atoms. Our results show that when the NC is small, the PDOS depends on the location of the Si atoms. However, as the size of the NC becomes large enough, the PDOS of the alloy will "stabilize" and become independent of the distribution of the Si atoms. The results presented in this paper are obtained from the NC satisfying this condition and contains a total of 1147 atoms (diameter $d\sim 3.7$ nm for pure Ge decreasing to ~ 3.5 nm for pure Si) with varying fractions of Si.

III. RESULTS

Figures 1(a) and 1(b) show the computed PDOS for eleven SiGe alloy NCs all containing 1147 atoms but with Si concentrations x varying from 0 (Ge) to 1 (Si). These figures are plotted in the same scale for easy comparison. From these calculations we have identified three main optical phonon peaks in the PDOS and extracted information on their frequencies, peak widths and heights as a function of x. The results are listed in Table I. In the literature, the two peaks with frequencies around 290 and 480 cm^{-1} have been identified as due to Ge-Ge and Si-Si bond vibrations from their proximity to the optical phonon frequencies of the pure bulk materials, and the peak with frequencies intermediate between them (around 400 cm^{-1}) has been attributed to the vibration of the Si-Ge bonds.[6,7] Since we can compute the vibration amplitudes of all the atoms of the NC for each eigenmode, we have used these results to investigate the microscopic details of these three main optical peaks.

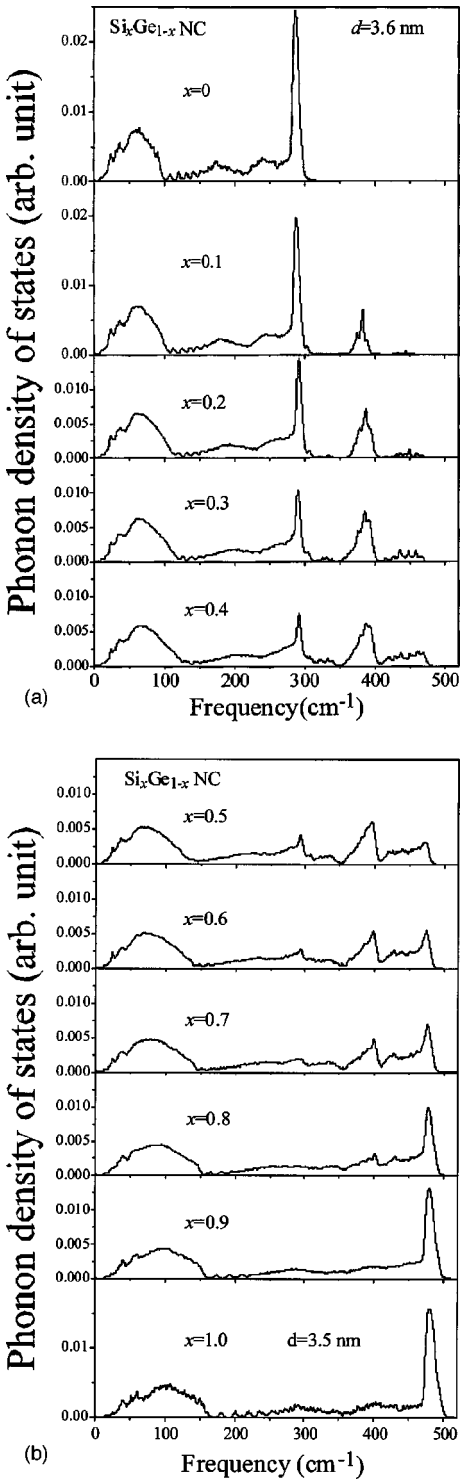

FIG. 1. The calculated phonon density-of-states (PDOS) in spherical SiGe NC with total number of atoms $N=1147$ ($d\sim 3.6$ nm) for Si concentration x equal to (a) 0 to 0.4 and (b) 0.5 to 1.

To facilitate our understanding of the behavior of phonons in alloy NCs, instead of presenting all the wealth of informa-

TABLE I. The frequencies (P), width (W), and height (H) of the three peaks: Ge, SiGe, and Si in the phonon density of states (PDOS) for Si_xGe_{1-x} alloy NC, calculated as a function of the Si fraction x. The peak positions and widths are given in unit of cm^{-1}. The unit for H is in arbitrary units.

x	P(Ge)	W(Ge)	H(Ge)	P(SiGe)	W(SiGe)	H(SiGe)	P(Si)	W(Si)	H(Si)
0.1	288.0	9.2	0.020	383.0	5.1	0.0066	444.6		0.0005
0.2	292.2	8.6	0.014	387.4	20	0.0072	450.0		0.0013
0.3	291.1	8.3	0.010	385.8	22	0.0074	436.0		0.0018
0.4	292.4	8.5	0.0077	387.2	23	0.0062	460.8		0.0022
0.5	293.7	23	0.0043	395.7	24	0.0061	469.9		0.0032
0.6	294.5	35	0.0028	397.5	23	0.0054	473.5	16.3	0.0055
0.7	291.9	89	0.0020	398.8	16	0.0048	475.5	15.3	0.0070
0.8				400.2	34	0.0032	476.9	13.7	0.0099

tion contained in our calculation, we will define a physical quantity known as the vibration-amplitude-squared (VAS) which is related to atomic vibration amplitude. For each single phonon mode, the sum of the VAS of all atoms is normalized to one. From the calculated VAS of each mode, we can select the single atom that has the maximum value of VAS (to be abbreviated as MVAS) and plot the MVAS as a function of the phonon frequencies. Much useful information about the NC phonon mode can be obtained from these plots. For example, if the MVAS of one mode is close to unity, this mode must be highly localized, since this indicates that only one atom vibrates very strongly at this frequency and all the other atoms are almost still. Conversely, if the MVAS is much less than 1, it implies a large number of atoms are involved in the vibration of this mode. In particular, if the MVAS is close to the inverse of the number of atoms in the NC, it indicates that all the atoms in the NC have nearly the same vibration amplitudes. Such plots have been shown to be useful in studying surface vibrational modes of Ge NC as distinct from those involving atoms lying in the interior.[15]

In case of a binary alloy we have separately plotted the MVAS for the two different types of atoms (Si or Ge) presenting in the alloy to highlight their different behaviors. Examples of such plots are shown in Figs. 2 and 3 for NCs with two alloy compositions $x=0.1$ and 0.6, respectively. In Figs. 4 and 5 the MVAS of the Si and Ge atoms in the same two alloys are separated according to their different locations, surface atoms as opposite to "body" atoms lying in the interior of the NC. In this paper we have defined surface atoms as atoms containing at least one dangling bond. Finally, in Figs. 6 and 7 the MVAS of both Si and Ge atoms are further separated according to their nearest neighbor configurations in order to investigate the relation between the vibration frequency of an atom and its local environment. Each interior atom, whether Si or Ge, has four nearest neighbors, so each atom with the MVAS can have up to five different combinations of nearest neighbors. It should be noted that we have treated *only interior* atoms here, i.e., the summation of all the MVAS in Figs. 6 and 7 should be equal to the upper panel of Figs. 4 and 5, respectively. The lower panels of Figs. 4 and 5 which correspond to the MVAS of *surface* atoms (which have at least one dangling bonds) are not included in Figs. 6 and 7.

IV. DISCUSSIONS

In this section, we will discuss our results and compare them with available Raman measurements. Because the Si atoms are randomly distributed, the NC does not have the same symmetry as the pure samples and as a result all the alloy vibrational modes are Raman active. For ease of discussion we will divide the PDOS into different regions according to their frequencies and discuss them separately.

A. Surface "acoustic" peaks in the PDOS

In the low frequency range (<100 cm^{-1}) of Figs. 1(a) and 1(b), we noticed that the PDOS consists of essentially one broad peak with a high frequency cutoff. In pure Ge NC this cutoff occurs around 100 cm^{-1}. Examination of the PDOS in bulk Ge indicates that the phonon modes in this region correspond to the transverse acoustic (TA) branches. As the concentration of Si (x) increases, both the center of this peak and

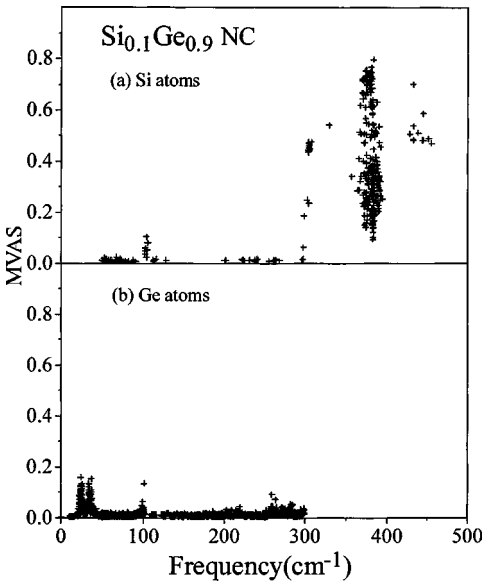

FIG. 2. Plot of the displacement amplitude-squared (AS) of the atom whose value of AS has the maximum value (or MVAS) versus the mode frequency for the alloy $Si_{0.1}Ge_{0.9}$. The atoms are further separated according to whether they are (a) Si or (b) Ge atoms.

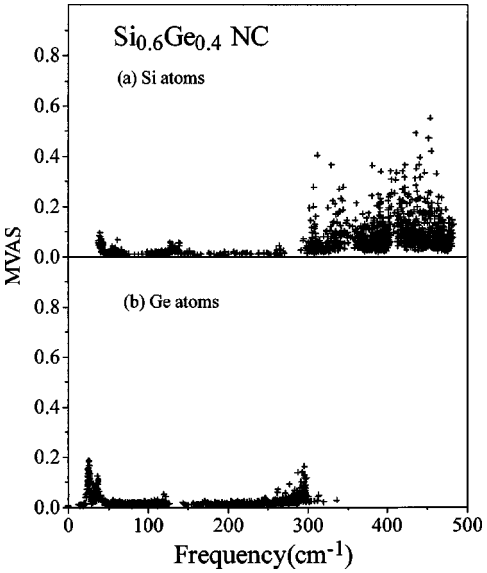

FIG. 3. Plot of the displacement amplitude-squared (AS) of the atom whose value of AS has the maximum value (or MVAS) versus the mode frequency for the alloy $Si_{0.6}Ge_{0.4}$. The atoms are further separated according to whether they are (a) Si or (b) Ge atoms.

its high frequency cutoff shift to higher frequencies and finally approaches the corresponding values in bulk Si. Superimposed on this broad peak are two relatively sharp peaks at the low frequency side that are present for nearly all NCs independent of Si concentrations. For $x<0.8$, their frequencies are about 24 and 38 cm^{-1}. In a separate publication on Ge NC,[15] we have identified two similar peaks in pure Ge NC as due to surface modes. These surface modes become, in the limit when the NC size becomes large, respectively, the torsional and spheroidal distortion modes of a homogeneous sphere predicted theoretically by Lamb,[18] and their frequencies will be represented by ω_t (torsional) and ω_s (spheroidal), respectively. The NC size ($d\sim3.6$ nm) in the present study is near the limit of NC size where the Lamb

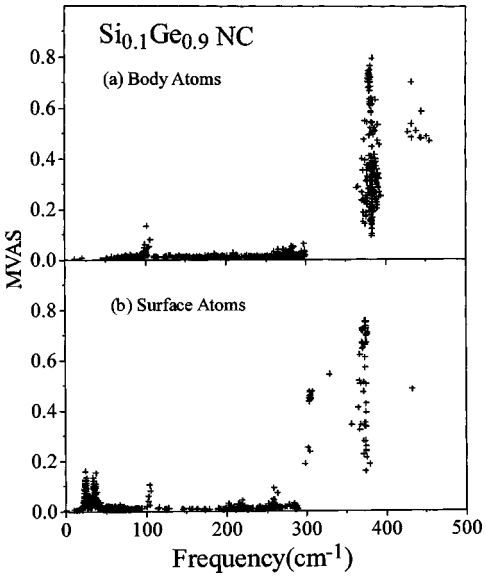

FIG. 4. Plot of the displacement amplitude-squared (AS) of the atom whose value of AS has the maximum value (or MVAS) versus the mode frequency for the alloy $Si_{0.1}Ge_{0.9}$. The atoms are further separated according to whether they are (a) body or (b) surface atoms.

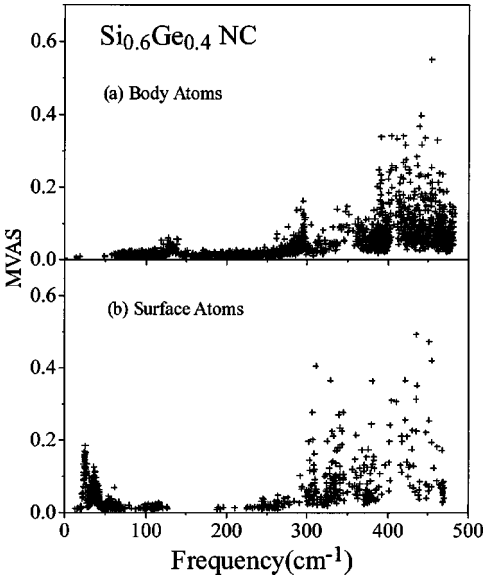

FIG. 5. Plot of the displacement amplitude-squared (AS) of the atom whose value of AS has the maximum value (or MVAS) versus the mode frequency for the alloy $Si_{0.6}Ge_{0.4}$. The atoms are further separated according to whether they are (a) body or (b) surface atoms.

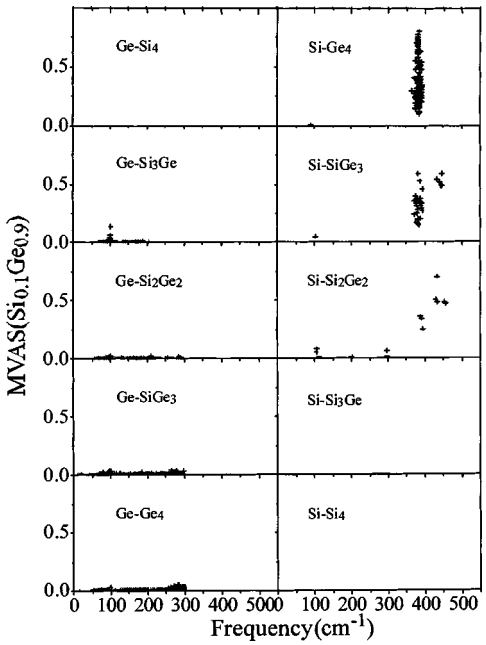

FIG. 6. Plot of the displacement amplitude-squared (AS) of the atom whose value of AS has the maximum value (or MVAS) versus the mode frequency for the alloy $Si_{0.1}Ge_{0.9}$. The atoms are separated according to whether they are Ge or Si atoms. The left-hand side column shows the Ge atoms surrounded by different numbers of Ge atoms while the right-hand side column shows the Si atoms surrounded by different numbers of Ge atoms.

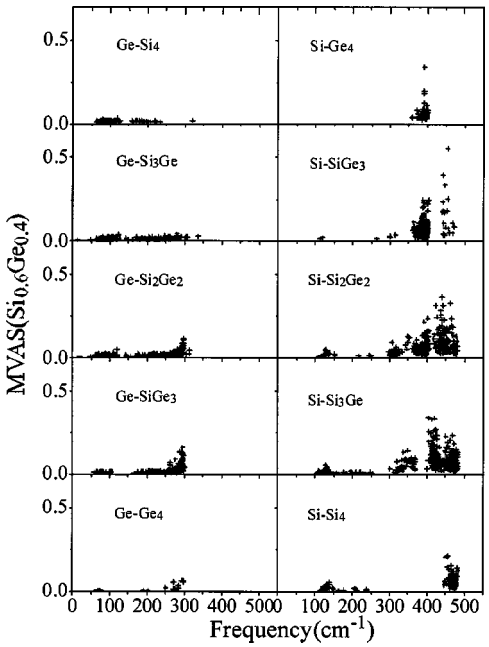

FIG. 7. Plot of the displacement amplitude-squared (AS) of the atom whose value of AS has the maximum value (or MVAS) versus the mode frequency for the alloy $Si_{0.6}Ge_{0.4}$. The atoms are separated according to whether they are Ge or Si atoms. The left-hand side column shows the Ge atoms surrounded by different numbers of Ge atoms while the right-hand side column shows the Si atoms surrounded by different numbers of Ge atoms.

theory is still valid for understanding the frequency of these low frequency surface modes. One characteristic of the Lamb surface modes is that their frequencies scale as the inverse of the diameter of the sphere and linearly with the acoustic phonon velocities. These Lamb's modes have been observed experimentally in several NC.[19,20] Figure 1 shows that these surface acoustic modes also exist in alloy NC. This can be verified directly by checking Figs. 4 and 5 where the MVAS of surface atoms also show two sharp peaks at the same frequencies. We found that as x changes in the alloy NC the frequencies of these surface acoustic phonons remain more or less the same as those of the pure Ge NC until x reaches 0.7. There is also no obvious change in the widths and heights of those two peaks. However, when x becomes >0.8, they are replaced by two peaks with frequencies equal to ~ 38 and $\sim 60\ \mathrm{cm}^{-1}$. We attributed these peaks to "Si dominated" surface acoustic modes of NC. These results suggest that the dependence of the two Lamb modes on the alloy composition in SiGe NC is similar to the "two-mode behavior" of optical phonons in bulk alloys.[21] We note that at $x=0.8$ [Fig. 1(b)] there is only one peak due to surface acoustic modes in the PDOS spectrum. We think this peak results from an accidental coincidence when ω_s of Ge happens to overlap with ω_t of Si. The behavior of these surface modes can be further understood by noting that the "Si dominated" surface modes are strongly hybridized while the reverse is not necessarily true. This results from the fact that for NC of a given size, there is a low frequency cutoff in the vibration modes. Since Si atoms are lighter than Ge atoms, this cutoff frequency is higher for pure Si NC than for Ge. In SiGe alloy NC, this cutoff frequency is determined mainly by the heavier Ge atoms. For SiGe NC with $x<0.5$, the frequencies of the "Si dominated" surface modes are higher than this cutoff frequency in a region where the PDOS is large, so the "Si dominated" surface modes are strongly damped. In the reverse case for alloys with larger values of x, this cutoff frequency will be determined mainly by Si atoms. Since the frequencies of "Ge dominated" surface modes lie *below* the vibrational frequency of most Si modes, they occur in regions with low PDOS and therefore are not strongly damped. As a result the Ge surface modes persist up to values of x as large as 0.8.

According to Lamb's theory, the ratio of the lower frequency torsional modes (ω_t) in pure Ge and Si should be equal to the ratio of their TA phonon velocities v_t (equal to 3.6×10^5 and 5.9×10^5 cm/s in Ge and Si, respectively) and is equal to 0.61. The corresponding ratio of the spheroidal modes (ω_s) would be given by the ratio of some linear combination of v_t and the longitudinal acoustic phonon velocities v_l (equal to 5.5×10^5 and 9×10^5 cm/s in Ge and Si, respectively). Since the ratio of v_l in Ge and Si turns out to be equal to 0.61 also the ratios of both ω_t and ω_s for pure Ge and Si from the Lamb theory are 0.61. These ratios from our calculated PDOS are both equal to 0.63, in good agreement with Lamb's theory.

B. Optical phonon modes in the PDOS

The frequency range from ~ 300 to $500\ \mathrm{cm}^{-1}$ in bulk samples is dominated by the optical phonon branches. We shall therefore refer to this frequency range as the "optical phonon range." As we discussed in Sec. III, this range is usually divided into three regions in the literature: the bulk Ge optical phonon region around $300\ \mathrm{cm}^{-1}$, the bulk Si optical phonon region around $500\ \mathrm{cm}^{-1}$, and the "so-called" Si-Ge vibration region around $400\ \mathrm{cm}^{-1}$. Based on our theoretical investigation our understanding of these peaks is presented below. Our results are compared with the experimental measurements in bulk SiGe alloy reported by Renucci *et al.*[6] and SiGe thin films and superlattices by others.

1. Ge optical phonon peak

Based on the results of our calculation [see Figs. 1(a) and 1(b) and Table I], we found that the Ge vibration mode spectrum shows little change with the increase in the number of Si atoms except for a rapid decrease in the strength of the Ge optical phonon peak around $300\ \mathrm{cm}^{-1}$. This peak blueshifts slightly as x increases. While the decrease in strength agrees with the experimental measurements [6,7] the experimental Ge phonon peak frequency in bulk alloy shows a *redshift* with an increase in x rather than a slightly blueshift predicted by our calculations. Two factors influence the frequency of this peak in our understanding. First, the contraction of the Si-Ge alloy lattice constant by Vegard's law would cause a blueshift of the peak, and second, the increasing localization of Ge optical modes due to the increasing amount of Si would cause a redshift of this peak. One effect which has been neglected in our simple model is the softening of the

Ge-Ge bonds caused by Si atoms. This discrepancy between theory and experiment suggests that the Vegard's Law might have over estimated the effect of decreasing lattice constant in the alloy. Experimentally the width of the Ge optical phonon peak *increases* with x. The calculated peak width decreases slightly as x increases to 0.5 but increases dramatically when $x > 0.5$, due to an overlap between the Ge optical phonon mode with the Si modes as well as SiGe modes leading to a broad tail on the low energy of the peak. It is difficult to make a direct comparison between theory and experiment since we have defined the peak width as the full width at half maximum of the strongest peak in the PDOS in this region. This definition which does not separate the sharp peak from its tail may not be the same as the one used in the experiments.[6,7]

2. Si-Ge optical phonon peak

Figures 2 and 3 show that while the Ge atoms dominate vibrational peaks with frequencies around and below 300 cm^{-1}, Si atoms dominate modes with frequencies above 300 cm^{-1}. In general, no Ge atoms have the MVAS for modes with frequency above 300 cm^{-1}. In the Si dominated optical phonon frequency range, we can further identify the following four distinct frequency ranges in Figs. 1–3 and 6–7: (i) ~330 cm^{-1}, (ii) ~390, (iii) ~430, and (iv) ~480 cm^{-1}. In particular Fig. 1 shows that the peak in region (ii) tends to be the strongest one for almost all alloy concentrations. The experimental frequency of this mode is 395 cm^{-1} for small values of x and it is usually referred to as the Si-Ge peak in the Raman spectra of SiGe alloys and superlattices. Examination of Figs. 2, 3, 6, and 7 suggests that this peak is due entirely to the vibration of Si atoms that are surrounded by more than two Ge atoms. Furthermore the large value of MVAS indicates that the vibration is strongly localized on the Si atom. In particular from Fig. 6 we see that, in $Si_{0.1}Ge_{0.9}$, the major peak occurs at 383 cm^{-1}, and is mainly from Si atoms surrounded by *four* Ge atoms with only small contributions from Si atoms surrounded by two to three Ge atoms. From our calculation (see Table I), we found that this peak blueshifts from 383 to 400 cm^{-1} as x increases. In $Si_{0.6}Ge_{0.4}$ (see Fig. 7) the major Si-Ge peak occurs at ~397 cm^{-1}, and the MVAS atoms have similar local environment as $Si_{0.1}Ge_{0.9}$, i.e., Si atoms are surrounded by two or more Ge atoms. The slight blueshifts in peak frequencies are caused by the variation in the number of neighboring Si atoms. The Si-Ge local mode peak totally disappears when x is greater than 0.9 because very few Si atoms would now be surrounded by two or more Ge atoms. It is interesting to contrast the different behavior of the vibrational modes of clusters with Si at its center ($Si\text{-}Ge_4$, $Si\text{-}SiGe_3$, $Si\text{-}Si_2Ge_2$, and $Si\text{-}Si_3Ge$), from those with Ge at its center ($Ge\text{-}Si_4$, $Ge\text{-}GeSi_3$, $Ge\text{-}Ge_2Si_2$, and $Ge\text{-}Ge_3Si$) in Figs. 6 and 7. For the latter cluster there are no localized phonon mode since these modes overlap with the Si vibrational frequencies and become resonant modes.

Another thing we notice from Figs. 1 is that, as x increases, the Si-Ge peak appears to broaden asymmetrically with a large width on the high energy side (the numerical results are shown in Table I). Its strength increases only slightly, reaches a maximum value, and then decreases as x becomes greater than 0.5. This broadening with x can be explained by the fact that, as x increases, more Si atoms form Si-Si clusters (i.e., cluster containing one or more than one pair of neighboring Si atoms). Figure 7 shows that the vibrational modes of such $Si\text{-}Si_2Ge_2$ and $Si\text{-}SiGe_3$ clusters can have both lower and higher frequencies than the frequency of the local mode of isolated Si atoms. An examination of Fig. 5 suggests that the surface Si-Si clusters with their dangling bonds tend to contribute to the lower frequency side in region (i) with frequency centered ~330 cm^{-1}. On the other hand the body clusters tend to dominate the higher frequency region (iii) with frequency centered around ~430 cm^{-1}. The weight of these body cluster modes is larger since there are more clusters in the interior of the NC. Modes in both regions (i) and (iii) exhibit large inhomogeneously broadening as a result of the statistical variations in the configuration of these Si-Si clusters.

3. Si-Si optical phonon peak

Figure 1 shows that for $x > 0.5$ a sharp peak appears in the frequency region (iv) at around 480 cm^{-1} and its height increases rapidly and width decreases slightly as x increases. Figure 7 shows that this frequency is associated with Si clusters containing no Ge atoms and is therefore related to the optical phonon mode in bulk Si. The frequency of this peak blueshifts as the Si concentration increases due to two factors: (1) it blueshifts as a result of the decrease in the average lattice constant when more Si is introduced and (2) more and larger Si clusters appear in the alloy when the amount of Si increases and this causes the vibrational frequency of the cluster to shift towards that of the bulk Si optical phonon.

C. Comparison with experiments

Our theoretical results can help with the interpretation of experimental Raman results in both bulk and NC of SiGe. For example, in NC the effect of confinement has been recognized to produce a redshift of the Raman modes. On the other hand we have shown that dangling bonds on the surface of the NC can also produce surface phonon modes with frequencies lower than those in the bulk. In SiGe NC we found that the localized Si-Ge peaks contain more information on the local environment of the Si atoms than the other phonon modes. In particular, the modes on the lower frequency side of this peak indicates the presence of Si atoms near the surface of the NC while peaks on the higher frequency side suggest the existence of cluster containing more than one Si atoms within the interior of the NC. In strained-layer superlattices and also thick epilayers of SiGe alloys grown on Si substrates, relatively sharp peaks have been found in the Raman spectra at around 255 and 435 cm^{-1}.[16] These peaks have been attributed to the presence of long-range ordering of Si and Ge planes along the [111] direction. If the ordering involves the formation of a new "supercell" consisting of two layers of Si and two layers of Ge as suggested by Ourmazd and Bean[22] then the sample will be dominated by only two kinds of clusters: $Si\text{-}Si_3Ge$ and $Ge\text{-}Ge_3Si$. From Figs. 6 and 7 we found that indeed

Si-Si_3Ge clusters will produce a peak in the PDOS around 420 cm^{-1}. We conclude that the Si-Ge optical phonon peak at about 430 cm^{-1} is formed by the Si-Si_3Ge clusters whose number is enhanced by the long-range ordering present in some samples. We also found that the vibration modes of Ge-Ge_3Si clusters cover a range of frequencies including the 255 cm^{-1} region but there are no sharp peaks in the PDOS. However, this does not preclude the possibility of a peak in the Raman cross section since the long-range ordering will affect the electronic wave functions leading to the enhancement of the Raman cross section of specific modes.

So far there have been very few experimental results on the phonon modes in SiGe NC. On the other hand extensive experimental Raman result in bulk SiGe alloys is available. Since we know that the NC surface affects mainly either the low frequency region or the frequency region slightly above the optical mode of Ge we can still utilize our results to understand the experimental Raman spectra in bulk SiGe alloys in the higher frequency regions. To compare our theoretical results with the experimental results reported by Renucci *et al.*[6] we have plotted in Fig. 8 the experimental Raman spectra of SiGe alloy on top of the theoretical PDOS for comparable values of x. In making these comparisons we should keep in mind that the theoretical frequencies for the peaks identified as "Si-Si" and "Ge-Si" by Renucci *et al.*[6] (straightly speaking the so-called Ge-Si peak is really due to Si atomic vibration as we have shown) will be slightly lowered than those in the experimental spectra because of our approximation in using the Ge force constants for even Si atoms. In addition our PDOS does not include the electron-phonon interaction necessary for calculating the intensity. Because of these limitations our calculation cannot reproduce some of the quantitative results obtained by Renucci *et al.*[6] such as the dependence of the peak position on the alloy concentration. Otherwise our computed PDOS agrees in general quite well with the experimental Raman spectra shown in Fig. 8. For example, Renucci *et al.*[6] found that for $x=0.54$ and 0.76 the "Ge-Si" Raman peak broadened asymmetrically while another broad peak appeared at 430 cm^{-1} and grew with x. Our calculations suggest that the peak at 430 cm^{-1} originates from the vibration of small Si clusters in the alloy in which a Si atom is surrounded by one to three Si atoms. The width of this peak is caused by inhomogeneous broadening of the vibration frequencies resulting from the different configurations of these clusters. Our interpretation of this peak is thus different from the local phonon mode of a Si embedded in the $Si_{0.5}Ge_{0.5}$ alloy model proposed by Renucci *et al.*[6] We also note that Tsang[23] has reported the Raman spectra of ultra-thin (less than 6 monolayer or ML) Ge film grown on Si [100] surface. According to our model the Si atoms at the film interface will have very well-defined local configuration: Each Si will be surrounded by two Si and two Ge atoms and therefore will be even narrower than the Si-Si_2Ge_2 spectrum shown in Fig. 7. Indeed the experimental spectra for the 2–3 and 5–6 ML (Ref. 23) show mainly one sharp peak without the higher energy tail due to Si cluster containing more than two Si atoms in the nearest neighbor. On the other hand, the thinnest 1 ML Ge thin shows two broad peaks indicating a lot of intermixing between Si and Ge atoms to form many clusters of different

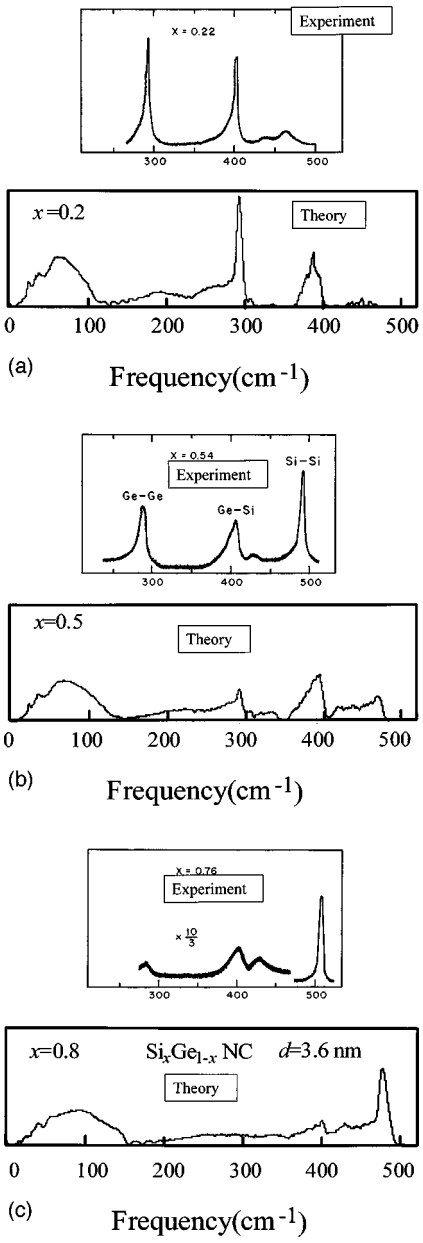

FIG. 8. Comparison between the theoretical phonon density-of-states (PDOS) calculated for NC and the experimental Raman spectrum in bulk SiGe alloy (Ref. 6) with comparable Si concentration x for (a) $x\sim0.2$, (b) $x\sim0.5$, and (c) $x\sim0.8$

configurations. Such intermixing induced broadening of the Ge-Si mode in experimental Raman spectra have also been reported in Ge/Si superlattice by Headrick *et al.*[4] and by Kwok *et al.*[2] in self-organized Ge quantum dots superlattice grown on Si substrates. When the superlattices are grown without a Sb surfactant layer these authors found that the Si local phonon peak around 417 cm^{-1} exhibits strong asymmetric broadening on the lower frequency side. Based on our calculation this result can be explain by the infiltration of Ge atoms into the Si barrier layers producing Si clusters with three or more Ge atoms. As in the case of the ultra-thin Ge films,[23] the Si local phonon peak in a perfect quantum dot film should be very sharp and results from the vibration of

$Si\text{-}Si_2Ge_2$ cluster only. Figures 6 and 7 show that the presence of clusters containing more Ge atoms such as $Si\text{-}SiGe_3$ produce additional modes mainly on the lower energy side of the Si local phonon.

V. SUMMARY AND CONCLUSIONS

In summary, we have investigated in detail the phonon properties of spherical SiGe alloy NC with a total of 1147 atoms (about 3.6 nm in diameter) as a function of Si concentration. The properties of phonon modes, including both vibration frequencies and vibration amplitudes, have been calculated directly by employing an average lattice constant following Vegard's rule. The phonon spectrum of the alloy NC is decomposed into different regions. The low frequency region (<300 cm^{-1}) is dominated by Ge vibrations that are the analogues of the acoustic and optical phonons in pure Ge samples, while the higher frequency region (>300 cm^{-1}) is dominated by the vibrational modes of Si atoms. Throughout most of the alloy series we found two low frequency peaks associated with surface vibrational modes superimposed on the broad continuum that were usually identified as the spheroidal and torsional modes of a continuum sphere. We have further identified that isolated Si atoms surrounded entirely by Ge atoms form a sharp localized phonon mode at 383 cm^{-1}, and vibrations of Si atoms in SiGe alloy NC produce a few bands of peaks centered around 330, 390, 430, and 480 cm^{-1}. These peaks are produced, respectively, by vibrations of surface Si atoms and Si clusters, localized vibration of Si atoms surrounded by mostly Ge atoms, vibration of Si atoms surrounded by more less equal numbers of Ge and Si atoms, and vibration of Si atoms surrounded mainly by Si atoms. From these results we understand that the so-called Ge-Si modes in the literature to be the localized phonon mode of isolated Si atoms in a Ge host. The vibrational modes of Ge atoms surrounded by Si atoms, on the other hand, do not produce localized phonons. Our theoretical phonons-density-of-states in NC have been found to explain qualitatively experimental Raman spectra in both bulk SiGe alloy samples and thin films of Ge grown on Si substrates.

ACKNOWLEDGMENTS

S.F.R. and W.C. are supported by the National Science Foundation (NSF0245648). W.C. is grateful to Illinois State University for hosting his visit. P.Y.Y. is supported in part by the Director, Office of Science, Office of Basic Energy Science, Division of Materials Sciences and Engineering, of the U.S. Department of Energy under Contract No. DE-AC03-76SF00098.

[1] A. D. Yoffe, Adv. Phys. **42**, 173 (1993); A. D. Yoffe, *ibid.* **50**, 1 (2001).
[2] See, for example, S. H. Kwok, P. Y. Yu, C . H. Tung, Y. H. Zhang, M. F. Li, C. S. Peng, and J. M. Zhou, Phys. Rev. B **59**, 4980 (1999) and references therein.
[3] See, for example, K. L. Teo, S. H. Kwok, P. Y. Yu, and S. Guha, Phys. Rev. B **62**, 1584 (2000) and references therein.
[4] R. L. Headrick, J.-M. Baribeau, D. J. Lockwood, T. E. Jackman, and M. J. Bedzyk, Appl. Phys. Lett. **62**, 687 (1993).
[5] R. Schorer, G. Abstreiter, S. de Gironcoli, E. Molinari, H. Kibbel, and E. Kasper, Solid-State Electron. **37**, 757 (1994).
[6] M. A. Renucci, J. B. Renucci, and M. Cardona, in *Proceedings of the International Conference on Light Scattering in Solids*, edited by M. Balkanski (Flammarion, Paris, 1971), p. 326.
[7] P. Yu and M. Cardona, *Fundamentals of Semiconductors, Physics and Materials Properties*, 3rd Ed. (Springer, Berlin, 2003).
[8] W. A. Harrison, *Electronic Structures and the Properties of Solids* (Freeman, San Francisco, 1980).
[9] S. F. Ren, Z. Q. Gu, and D. Lu., Solid State Commun. **113**, 273 (2000).
[10] S. F. Ren, D. Y. Lu, and G. Qin, Phys. Rev. B **63**, 195315 (2001).
[11] G. Qin and S. F. Ren, J. Appl. Phys. **89**, 6037 (2001).
[12] G. Qin and S. F. Ren, Solid State Commun. **113**, 273 (2000).
[13] W. Cheng and S. F. Ren, Phys. Rev. B **65**, 205305 (2002).
[14] S. F. Ren and W. Cheng, Phys. Rev. B **66**, 205328 (2002).
[15] W. Cheng, S. F. Ren, and P. Y. Yu, Phys. Rev. B **68**, 193309 (2002).
[16] D. J. Lockwood, K. Rajan, E. W. Fenton, J.-M. Baribeaue, and M. W. Denhoff, Solid State Commun. **61**, 465 (1987).
[17] L. Vegard, Z. Phys. **5**, 17 (1921).
[18] H. Lamb, Proc. London Math. Soc. **13**, 189 (1882).
[19] N. N. Ovsyuk, E. B. Gorokhov, V. V. Grishchenko, and A. P. Shebanin, JETP Lett. **47**, 298 (1988).
[20] A. Tanaka, S. Onari, and T. Arai, Phys. Rev. B **47**, 1237 (1993).
[21] L. Genzel, T. P. Martin, and C. H. Perry, Phys. Status Solidi B **62**, 83 (1974).
[22] A. Ourmazd and J. C. Bean, Phys. Rev. Lett. **55**, 765 (1985).
[23] J. C. Tsang, in *Light Scattering in Solids V*, edited by M. Cardona and G. Güntherodt, Topics in Applied Physics, Vol. 66 (Springer, Berlin, Heidelberg, 1989), pp. 233–284.